

On the methods based on the Pressure Rise Test for monitoring a freeze-drying process

*Original*

On the methods based on the Pressure Rise Test for monitoring a freeze-drying process / Fissore, Davide; Pisano, Roberto; Barresi, Antonello. - In: DRYING TECHNOLOGY. - ISSN 0737-3937. - STAMPA. - 29:1(2011), pp. 73-90. [10.1080/07373937.2010.482715]

*Availability:*

This version is available at: 11583/2342419 since:

*Publisher:*

TAYLOR & FRANCIS INC

*Published*

DOI:10.1080/07373937.2010.482715

*Terms of use:*

This article is made available under terms and conditions as specified in the corresponding bibliographic description in the repository

*Publisher copyright*

(Article begins on next page)

This is an electronic version (author's version) of an article published in DRYING TECHNOLOGY, Volume 29, Issue 1, pages 73-90 (2011).

DRYING TECHNOLOGY is available online at:

<http://www.tandfonline.com/openurl?genre=article&issn=0737-3937&volume=29&issue=1&spage=73>

## **On the methods based on the Pressure Rise Test for monitoring a freeze-drying process**

Davide Fissore<sup>\*</sup>, Roberto Pisano, Antonello A. Barresi

*Dipartimento di Scienza dei Materiali e Ingegneria Chimica - Politecnico di Torino  
corso Duca degli Abruzzi 24, 10129 Torino (Italy)*

---

<sup>\*</sup> Corresponding author

phone: +39-011-0904693  
fax: +39-011-0904699  
e-mail: [davide.fissore@polito.it](mailto:davide.fissore@polito.it)

## **Abstract**

This paper is focused on the methods based on the Pressure Rise Test (PRT) used to monitor the primary drying of a lyophilisation process. Details about the model-based algorithms proposed to interpret the PRT, namely the Manometric Temperature Measurement (MTM), the Pressure Rise Analysis (PRA), and the Dynamic Parameters Estimation (DPE) are briefly summarized and various features of the models used by these algorithms, in particular the role of the vial wall and of radiation on the thermal balance of the system, are investigated. The optimal selection of the sampling frequency and of the time interval between two tests is discussed, and the influence of the duration of the test on the results is investigated by means of mathematical simulation: results obtained from the PRT can be significantly improved by optimizing the duration of the test. Moreover, the problem of misleading results obtained at the end of the primary drying is investigated, taking into account the problem of ill-conditioning of the algorithms. An improved version of the DPE algorithm is proposed to cope with this problem: its effectiveness is demonstrated by means of mathematical simulations and experimental runs.

## **Keywords**

- Freeze-drying
- Pressure Rise Test
- Manometric Temperature Measurement
- Pressure Rise Analysis
- Dynamic Parameters Estimation

## Introduction

Product quality control in a freeze-drying process requires monitoring in-line the temperature and the residual water content of the product, both during primary drying, when frozen water is removed by sublimation, and during secondary drying, when the residual water, bound to the partially dried product, is desorbed.

Product temperature has to be carefully maintained below a limit value that is a characteristic of the product. In case of solutes that crystallize during freezing, the limit temperature corresponds to the eutectic point, in order to avoid the formation of a liquid phase, and the successive boiling due to the low pressure. In case of solutes that remain amorphous during freezing, the maximum allowed product temperature is close to the glass transition temperature, in order to avoid the collapse of the dried cake. In this case, limit temperature can be very low and is also dependent on the residual moisture.<sup>[1]</sup> The occurrence of the collapse of the dried cake can be responsible of a higher residual water content in the final product, of a higher reconstitution time and of the loss of activity of the pharmaceutical principle. Moreover, a collapsed product is often rejected because of the unattractive physical appearance.<sup>[2],[3],[4]</sup> In case heat is supplied (at least partially) from above, care has to be taken to avoid reaching scorch temperature in the upper part of the product.

The residual amount of frozen water has to be monitored during primary drying in order to detect the ending point of this stage: if secondary drying is started before the end of the previous step, the product temperature may exceed the maximum allowed value, thus causing melting or collapse, while if secondary drying is delayed, the cycle is not optimized and the cost of the operation increases. Finally, the residual water content at the end of secondary drying has to be monitored: for most products the target level is very low, usually from less than 1.0% up to 3.0%, even if, for certain products, it has been demonstrated that a too low level of residual water should be avoided and the final value must be in a well defined range.<sup>[5]</sup>

This paper is focused on the monitoring of the primary drying phase as this step is generally recognized to be the longest and the most risky phase of the whole process: the amount of bound water in the partially dried product is in fact higher during primary drying and, thus, the product temperature has to be maintained below a very low value. As a consequence, the duration of primary drying can be very high. On the contrary, higher temperatures are allowed during secondary drying because of the lower amount of residual moisture.

Monitoring of the primary drying is particularly difficult as it is not possible to measure in-line the product temperature and the residual water content without interfering with the process dynamics. Moreover, when pharmaceuticals are processed, sterile conditions can be impaired. Besides, the use of sensors in vials is allowed only in pilot scale equipment, while it is not feasible in production scale units with automatic loading/unloading systems. The state of the art of the techniques available to monitor primary drying has been recently reviewed and discussed by Wiggenhorn et al.<sup>[6]</sup>, by Barresi and Fissore<sup>[7]</sup>, and by Barresi et al.<sup>[8]</sup>, who described an innovative and modular monitoring system that can take advantage of redundancy and synergistic effects of different devices.

A widespread technique used for monitoring the primary drying is the Pressure Rise Test (PRT), firstly proposed by Neumann in 1961: the valve placed in the spool connecting the vacuum chamber to the condenser is closed for a short time period (typically 15-30 seconds) and the pressure inside the chamber increases, as a consequence of the accumulation of water vapor, at first rapidly and then more slowly when the chamber pressure approaches the equilibrium value with the ice surface. Chamber pressure data are collected during the PRT and related to the sublimating interface temperature using graphical methods, in early works, and mathematical models, in modern applications. The evolution of the product temperature can be monitored during the entire process if the PRT is performed different times during primary drying. Furthermore, the pressure rise gives also information on the entity of the sublimation flow, which is directly related to the slope of the pressure rise curve at the beginning of the PRT. Thus, it can potentially provide information concerning the passage from primary drying to secondary drying, characterized by the strong decrease of the vapor flow from the vials into the chamber.

The PRT has also been proposed to monitor in-line the moisture content in the product during the secondary drying. The saturation vapor pressure existing in the drying chamber after a shutting-off period was used by Neumann<sup>[9]</sup> to determine the residual moisture content: this requires the knowledge of the desorption isotherms of the material being dried, and, of course, that the equilibrium value is reached, which is not always feasible. A different method based on the estimation of the vapor flow from the PRT was proposed by Pikal et al.<sup>[10]</sup> and by Tang et al.<sup>[11]</sup>: it requires the knowledge of the actual moisture content at the end of primary drying. Fissore et al.<sup>[12]</sup> proposed a method that couples the measurement of water desorption rate with a mathematical model that describes the evolution in time of the residual water content in the dried product: by this way it is possible to estimate the evolution of the residual water content of the dried product without knowing the value of the water

concentration at the beginning of secondary drying.

The goal of this paper is to investigate some model-based methods using the PRT for monitoring the primary drying of a lyophilisation process, i.e. the Manometric Temperature Measurement<sup>[13],[10],[14],[15],[16]</sup>, the Pressure Rise Analysis<sup>[17]</sup>, and the Dynamic Parameters Estimation<sup>[18],[19]</sup>. The main features of these methods are the followings:

- a mathematical model is used to describe the pressure rise in the drying chamber during the PRT;
- the pressure in the drying chamber is measured during the PRT;
- an optimization algorithm is used to estimate the product temperature and the residual water content looking for the best fit between the pressure measurement and the values obtained by mathematical simulation. Also other parameters, e.g. the heat transfer coefficient between the shelf and the vials and the resistance of the dried product to vapor flow, can be estimated from the PRT: their values are required in case modern control tools, that allow for process optimization and preserve product quality, are used.<sup>[8],[20]</sup>

In the first part of the paper the characteristics of the various model proposed to describe the PRT are briefly summarized, and various features, in particular the role of the vial wall and the role of radiation on the thermal balance of the system, are investigated. It must be evidenced that all the proposed methods refer to the case where sublimation heat is supplied through the shelf below the product, which is the common case in pharmaceuticals production, and are not applicable in case of microwave or radiant heating. Then, the optimal selection of the sampling frequency and of time interval between two tests is discussed, and mathematical simulation is used to investigate the influence of the duration of the test on the results obtained. Accuracy can be significantly improved by selecting the optimal duration of the test, that is related to the characteristic time of the process. Moreover, the problem of misleading results obtained at the end of the primary drying is investigated, taking into account the problem of ill-conditioning of the algorithms, and an improved version of the Dynamic Parameters Estimation algorithm is proposed to cope with this problem: its effectiveness is demonstrated by means of mathematical simulations and experimental runs.

## **State of the art**

Early works<sup>[9],[21],[22],[23]</sup> proposed to use the transient pressure response measured during a

PRT for determining the end of primary drying, and for estimating the product temperature on the basis of the saturating vapor pressure of the ice. Oetjen proposed and patented a method, the Barometric Temperature Measurement (BTM), to estimate the temperature of the sublimating interface using the value of the pressure at which the first derivative of the pressure rise curve has a maximum<sup>[24],[25],[26]</sup>; the sublimation flow is calculated by the rate of pressure increase at the beginning of the test. Milton et al.<sup>[13]</sup>, Liapis and Sadikoglu<sup>[27]</sup>, Obert<sup>[28]</sup>, Chouvenec et al.<sup>[17]</sup>, and Velardi et al.<sup>[18]</sup> proposed to use mathematical models to estimate the temperature of the product, as well as some parameters of the system, on the basis of pressure rise data: what differentiates one algorithm with respect to the others is the mathematical model used and the parameters estimated. Details about these models are briefly summarized in the following.

### ***Manometric Temperature Measurement***

The Manometric Temperature Measurement (MTM) algorithm, originally proposed by Milton et al.<sup>[13]</sup>, assumes that the evolution of the pressure during the PRT is the consequence of four mechanisms:

- 1) direct sublimation of ice at a constant temperature,
- 2) product heating by the shelf during the PRT,
- 3) temperature equilibration across the frozen matrix,
- 4) leak in the chamber.

An equation consisting of the sum of the previous terms is proposed and the vapor pressure over the ice ( $p_{w,i}$ ), a parameter that is a function of the product resistance to vapor flow ( $K$ ), and the heat transfer coefficient between the bottom of the vial and the shelf ( $K_v$ ) are estimated by looking for the best fit between experimental values of pressure rise and mathematical simulation of the process. The interface temperature is calculated from  $p_{w,i}$  using thermodynamic vapor-ice equilibrium data.

An improved version of this algorithm was proposed by Pikal et al.<sup>[10]</sup> and by Tang et al.<sup>[11],[14],[15],[16]</sup>: they estimate  $p_{w,i}$ , the total resistance of the dried product and of the stopper to the vapor flow ( $\hat{R}_p + \hat{R}_s$ ), and a fitting parameter indicated with  $X$ . Differently from the algorithm proposed by Milton et al.<sup>[13]</sup>, they calculate the heat transfer coefficient  $K_v$  by equating the heat consumed by ice sublimation and the heat flow from the shelf to vials. Details about the MTM algorithms are given in Appendix 1.

Some hypothesis at the basis of the model can be potential source of errors, as discussed

by Milton et al.<sup>[13]</sup>:

- the frozen product is assumed to behave like a slab thermally insulated at both faces, while the sublimation interface is in contact with the porous matrix and the bottom part of the product is in contact with the vial;
- the temperature difference across the frozen product ( $\Delta T_i$ ) and the thickness of the frozen product ( $L_f$ ) are required to perform the calculations, but they are not exactly known:  $\Delta T_i$  is assumed to be constant and equal to 2°C, but an equation for the calculation of  $\Delta T_i$  as a function of  $p_c$ ,  $T_s$ , and of the parameters estimated by the MTM algorithm, has also been proposed;<sup>[15],[16]</sup>
- the role of the heat capacity of the vial wall is assumed to be negligible.

A modification of the MTM method was proposed by Obert<sup>[28]</sup>: it takes into account the heat capacity of the whole glass wall of the vial and the contribution of the desorption of the bound water to the pressure rise. The parameters that are estimated are  $T_i$ ,  $K$  (the same parameter of the MTM algorithm originally proposed by Milton et al.<sup>[13]</sup>), the leak rate, and the desorption rate of bound water.

### ***Dynamic Pressure Rise***

Liapis and Sadikoglu<sup>[27]</sup> proposed a more complex algorithm, called Dynamic Pressure Rise (DPR), to determine the temperature profile in the dried and in the frozen product from the PRT. The DPR algorithm is based on the unsteady-state mathematical model presented by Sadikoglu and Liapis.<sup>[29]</sup> Many parameters are needed to perform the analysis, e.g. the diffusivity and the permeability of the porous layer, the heat transfer coefficient between the bottom of the vial and the heating shelf, the temperature and the partial pressure at the top of the vial: as a consequence, the practical application in-line of this method is a complex task, even if feasible in theory.

### ***Pressure Rise Analysis***

Chouvenec et al.<sup>[17]</sup> proposed an algorithm, the Pressure Rise Analysis (PRA), based on a simple macroscopic heat balance for the frozen product, taking also into account the desorption of bound water and the thermal capacity of the portion of the vial glass in contact with the frozen product. The product temperature at the interface of sublimation, the resistance of the dried layer to vapor flow, and the desorption rate of bound water are estimated, even if the desorption rate is generally considered to be negligible. The temperature



at the bottom of the vial is assumed to remain constant during the PRT, even if the vial bottom is continuously heated during the process and the heat removal at the interface is reduced due to the increased chamber pressure which reduces the driving force for sublimation. Details about PRA algorithm are given in Appendix 2.

### ***Dynamic Parameters Estimation***

The Dynamic Parameters Estimation (DPE) algorithm proposed by Velardi et al.<sup>[18]</sup> and Velardi and Barresi<sup>[19]</sup> is based on an unsteady-state model for mass transfer in the drying chamber and on the energy balance for the frozen layer, thus taking into account the different dynamics of the temperature at the interface and at the vial bottom. The role of the vial wall in the thermal balance of the system during the PRT is assumed to be negligible. The temperature profile in the product and the mass transfer resistance to vapor flow in the dried layer are estimated. Moreover, expressions for the calculations of the heat transfer coefficient between the heating shelf and the vial, of the actual thickness of the frozen portion of the product, and of the solvent sublimation flow in the drying chamber are given. Details about DPE algorithm are given in Appendix 3.

### ***Analysis of the models used by MTM, PRA and DPE algorithms***

In this paragraph we focus on various features that characterize the MTM, PRA, and DPE algorithms. In particular, the most significant differences will be evidenced, and the influence of some important assumptions will be discussed with the support of the results obtained with a detailed model. The use of mathematical simulation of the process allows investigating accurately and reliably the relevance and consequences of different assumptions of the various models used to interpret the PRT and, thus, to compare the various algorithms: in fact, in this case, the values of the variables that are estimated through the identification procedure are exactly known.

Various mathematical models have been proposed in the Literature to describe the evolution of the product during a freeze-drying process. They can be divided into two groups, namely multi-dimensional models (see, among the others, Ref [30]) and mono-dimensional models (see, among the others, Ref. [31] and [34]). While the models of the former group take into account radial profiles of temperature in the frozen and dried product, and of composition in the dried cake, as well as the curvature of the interface of sublimation, these issues are neglected when using mono-dimensional models. Multi-dimensional models are quite complex, and their numerical solution can be highly time-consuming. Moreover, they involve

many parameters (e.g. tortuosity of the dried cake, dusty gas equation parameters, and many others) that are very often unknown, or that could be estimated with high uncertainty. Besides, it appears from published works that in typical lyophilization conditions radial thermal gradients are usually small, even when radiation from the environment is taken into account, and also the curvature of the interface is very limited.<sup>[30]</sup> This agrees with the results given by Pikal<sup>[31]</sup>, where it was found in a series of experiments that the temperature at the bottom centre of the vial was equal to the temperature of the bottom edge, within the uncertainty of the temperature measurement (0.5°C). This conclusion is also confirmed by recent papers showing results obtained solving a multi-dimensional model with a finite element method.<sup>[32],[33]</sup>

As far as mono-dimensional models are concerned, it has to be remarked that none of them included the effect of heat transfer in the sidewall of the vial, although it has been argued that this could play an important role in vial lyophilization.<sup>[35],[36]</sup> Recently, a mono-dimensional model including the transient energy balance to describe the heat transfer in the vial wall was proposed by Velardi and Barresi<sup>[37]</sup>. This model was validated using experimental data from a pilot-scale freeze-dryer, and very good predictions of the dynamics of the primary drying phase were obtained. For these reasons this model has been used for the calculations. In any case it must be evidenced that the results are substantially independent of the model adopted in case the model takes into account the main heat and mass transfer mechanisms and, in particular, heat conduction in the wall. The case study that will be analyzed in the following is the freeze drying of a 10% by weight sucrose solution in tubing vials having an internal diameter of  $14.25 \cdot 10^{-3}$  m ( $L_{f,0} 7.21 \cdot 10^{-3}$  m,  $p_c = 10$  Pa,  $T_s = -20^\circ\text{C}$ ,  $N_v = 200$  vials,  $V_c = 0.2$  m<sup>3</sup>). This case study can be considered representative of a wide number of industrial processes.

All the models used to describe the PRT require knowing the value of the thickness of the frozen layer. Both MTM and PRA algorithms estimate this value *a posteriori*, by considering constant sublimation flow between two subsequent PRTs: the value of  $L_f$  at the generic run is retrieved by subtracting to the total initial mass of frozen product the sum of the mass sublimated up to the time of the current PRT. This approach requires a high frequency of the test (e.g. every 30-60 minutes) in order to get good accuracy. In the DPE algorithm the ice thickness is calculated through a material balance written across the moving interface, which is solved with the equations of mass balance in the drying chamber and of heat balance in the frozen product. For a better accuracy the simplified model of Velardi and Barresi<sup>[37]</sup> can be used to calculate the time evolution of  $L_f$  and of  $T_i$  between to subsequent PRTs, but, in

order to reduce the computational demand, a quadrature formula was proposed to carry out the integration (details are given in Appendix 3).

With respect to the content of the freeze-dryer chamber, MTM algorithm assumes that it is 100% water vapor during primary drying, even if other gases are known to be present. PRA and DPE algorithms take explicitly into account the amount of inert gas that is present in the drying chamber, and that can be measured by means of a thermo-conductivity gauge (using also the measurement of a capacitive gauge) or of a laser analyzer.

It is well known that a batch of vials can exhibit a significant degree of heterogeneity as a consequence of radiation from the chamber walls (unless the batch is shielded), vapor fluid-dynamics in the chamber, and non-uniform distribution of the temperature of the heating shelf. A detailed discussion of these effects can be found in Barresi et al.<sup>[38]</sup> All the PRT based methods basically assume that the batch is homogeneous, but Velardi and Barresi<sup>[19]</sup> and Velardi et al.<sup>[18]</sup> introduced a correction coefficient, that can be estimated by DPE algorithm, to account for the heterogeneity of the vial batch.

All the methods require knowing the relation between the temperature of the sublimation interface and the equilibrium water pressure. The Goff-Gratch equation<sup>[39]</sup> for the vapor pressure over ice covers a range from -100°C to 0°C and is generally considered as the reference equation: it is recommended by the World Meteorological Organization<sup>[40]</sup>, and the values obtained using this equation are in perfect agreement with those given by the International Association for the Properties of Steam.<sup>[41]</sup> The use of the Goff-Gratch equation was proposed by Velardi et al.<sup>[18]</sup> in the formulation of the DPE algorithm (note that a typing mistake was present in Table 1 of Ref. 18):

$$p_{w,i} = 100 \cdot \exp \left[ -9.09718 \left( \frac{273.16}{T_i} - 1 \right) - 3.56654 \log_{10} \left( \frac{273.16}{T_i} \right) + \right. \\ \left. + 0.876793 \left( 1 - \frac{T_i}{273.16} \right) + \log_{10} 6.1071 \right] \quad (1)$$

Equation (1) can be simplified: it is possible to calculate the values of  $p_{w,i}$  in the temperature range of interest for freeze-drying, and then these values can be interpolated. This motivates the difference between the equations given by Pikal et al.<sup>[10]</sup> (2005) and by Tang et al.<sup>[14],[15],[16]</sup> for the MTM algorithm:

$$p_{w,i,MTM} = \frac{101325}{760} \left( e^{-\frac{6144.96}{T_i} + 24.01849} \right) \quad (2)$$

and by Chouvenec et al.<sup>[17]</sup> for the PRA algorithm:

$$p_{w,i,PRA} = e^{\frac{-6320.1517}{T_i} + 29.5578} \quad (3)$$

A simplified equation was also tested in previous applications of the DPE algorithm<sup>[8],[20]</sup>:

$$p_{w,i,DPE} = e^{\frac{-6140.4}{T_i} + 28.916} \quad (4)$$

Different values are obtained when using previous equations to calculate the vapor pressure at a given temperature: the difference can vary from -1.2 to 0.4 Pa at -40°C, and from -4.6 to 2.3 Pa at -20°C. Thus, when the interface temperature is retrieved from the pressure value, different values are obtained according to the equation used. In the followings, when results obtained using the various algorithms will be compared, eq. (4) will be used for all the methods in order to avoid the influence of a different choice for the interpolation function.

With respect to the role of the vial wall in the thermal balance of the system, it can be relevant during the primary drying (see, among the others, Schelenz et al.<sup>[43]</sup>; Brülls and Rasmuson<sup>[36]</sup>, Hottot et al.<sup>[32]</sup>, Velardi and Barresi<sup>[37]</sup>, Brülls and Rasmuson<sup>[33]</sup>). Actually, as said before, it has been proven that the effect of the vial wall, with respect to the heat conduction in the axial direction and to the radial flux from the chamber wall, can be accounted for in a one-dimensional model by using an effective heat transfer coefficient.<sup>[37]</sup> This is also true for the PRT. Figure 1 shows the evolution of pressure in the drying chamber and of the product temperature at the bottom of the vial as a function of time during three PRTs at 25%, 50% and 75% of the total primary drying time: these values have been calculated by means of mathematical simulation taking into account the effect of the glass wall, or neglecting it and using an effective heat transfer coefficient between the shelf and the product at the bottom of the vial. The value of the effective heat transfer coefficient has been calculated using the following procedure: firstly, the evolution of the system has been calculated using the mathematical model that accounts for the role of the vial; then, results have been compared with those obtained with a second model, where thermal balance at the wall is not considered. Finally, the value of the heat transfer coefficient used by the second model was modified, looking for the best fit with the results obtained with the first model. Radiation from chamber walls is neglected, in order to focus on the effect of the glass wall. Results evidence that the use of an effective value for  $K_v$  is able to take into account the effect of the wall of the vial and, thus, it is not necessary to include the vial heat capacity in the energy balance. As a consequence, the heat transfer coefficient obtained using the various algorithms proposed to interpret the PRT has to be regarded as an effective coefficient, as the models used by those algorithms neglect the thermal dynamics of the wall.

With respect to the role of the radiation from the chamber wall, it affects the dynamics of a very low number of vials (only 6-7% of the vials of a batch in an industrial apparatus are affected by radiation as they are placed at the side of the tray) while in a small-scale apparatus, used for R&D purposes, the problem should be avoided by proper shielding. Radiation from the upper tray affects uniformly the vials of the batch, but the effect is generally reduced by the presence of the stopper that, at least partially, shields the product. Again, the effect of radiation can be accounted for by using an effective heat transfer coefficient. Figure 2 shows the time evolution of pressure in the drying chamber and of the product temperature at the bottom of the vial during three PRTs at 25%, 50% and 75% of the main drying: these values have been calculated by means of mathematical simulation taking into account uniform radiation from the upper tray, or neglecting it and using an effective heat transfer coefficient between the shelf and the product at the bottom of the vial. Results refer to the same case study previously considered to assess the effect of the glass wall, but now the dynamics of the glass wall is neglected in order to focus on the effect of radiation. Results evidence that the use of an effective value for  $K_v$  is able to take into account the effect of radiation, if it is limited, and, thus, when radiation is neglected in the model used to describe the PRT, an effective value of  $K_v$  is obtained.

The heat transfer coefficient  $K_v$  is a function of chamber pressure, but the effect of this variation during the PRT has been considered negligible by previous authors. Figure 3 shows that the evolutions of chamber pressure and product temperature during some PRTs calculated taking into account the variation of  $K_v$  with the pressure are in good agreement with those calculated assuming a constant value of  $K_v$ : the maximum difference between the two curves (of chamber pressure and product temperature) is at the end of the PRT, and is lower than 2% for chamber pressure, and of 0.5% for product temperature. Results refer to the same case study previously considered to assess the effect of the glass wall and of radiation, but now both issues have been neglected in order to focus on the effect of the influence of  $p_c$  on  $K_v$ .

### **Optimal selection of the sampling frequency and of the time interval between two PRTs**

All the methods based on the PRT can be regarded as nonlinear parameters estimation tools, where the interface temperature at the beginning of the test ( $T_i$ ), or the vapor pressure at the sublimating interface ( $p_{w,i}$ ), and the product resistance ( $R_p$ ), or the average vapor diffusivity in the dried layer ( $k_1$ ), are calculated in order to minimize the difference between the measured

$(p_{c,meas})$  and the calculated  $(p_c)$  values of chamber pressure: a nonlinear least-square optimization problem is solved:

$$\min_{p_{w,i}, k_1} \sum_k (p_{c,k} - p_{c,meas,k})^2 \quad (5)$$

Values of chamber pressure during the PRT have to be collected using an adequate sampling frequency. A rule of thumb that is generally given when collecting experimental data for process identification is that the sampling interval should be not higher than 0.1-0.2 times the time constant of the process. A simplified approach can be used to calculate the time constant. During the PRT the pressure evolution in the chamber can be described by the following equation:

$$\left( \frac{V_c}{T_c} \right) \frac{dp_{w,c}}{dt} = \frac{k_1 N_v A_p}{T_i (L - L_f)} (p_{w,i} - p_{w,c}) \quad (6)$$

and, assuming that  $T_c = T_i$ , we obtain:

$$\frac{V_c (L - L_f)}{k_1 N_v A_p} \frac{dp_{w,c}}{dt} + p_{w,c} = p_{w,i} \quad (7)$$

As an alternative, approximate chamber temperature can be calculated from shelf temperature and interface temperature:

$$T_c = \frac{1}{2} (T_s + T_i) \quad (8)$$

and, after some manipulations, we obtain:

$$T_c = T_i + \frac{1}{2} (T_s - T_i) = T_i \left( 1 + \frac{1}{2} \frac{T_s - T_i}{T_i} \right) = T_i (1 + \zeta) \quad (9)$$

where  $\zeta \ll 1$  (as an example, in case  $T_s = 263$  K and  $T_i = 243$  K,  $\zeta$  is about 0.04) and, thus, eq. (7) is still valid. The variation of the thickness of the frozen layer during the PRT is negligible, while  $T_i$  (and, thus,  $p_{w,i}$ ) slightly changes, even if its variation is generally lower than 0.5-1°C. If  $T_i$  is assumed to remain constant during the test, which can be accepted in the framework of this analysis, then eq. (7) describes the dynamics of a first order system, whose time constant is given by:

$$\tau = \frac{V_c (L - L_f)}{k_1 N_v A_p} \quad (10)$$

Equation (10) can thus be used to estimate the time constant of the process and, then, the optimal sampling frequency of the values of chamber pressure. The use of eq. (10) requires knowing the value of  $k_1$ : a first guess of this value can be obtained from the Literature, or it

can be estimated from the first PRT.

With respect to the time interval between two PRTs, it has to be taken into account that the only parameter of the model that is affected by the time interval between two tests is  $L_f$ . If we assume to be at a generic time  $t_j$  where a PRT is performed, then the value of frozen layer thickness is obtained by taking the value of  $L_f$  estimated in the previous test ( $t_{j-1}$ ) and then subtracting the mass of ice sublimated in the time interval  $t_j - t_{j-1}$ : this value is calculated by the time integration of the sublimation flow estimated at time  $t_{j-1}$ . Thus, if the sublimation flow does not vary between the two PRT, as it is generally the case, the frequency of the tests does not affect the calculated value of  $L_f$  and, thus, the estimations of product temperature. If the sublimation flow changes because of collapse (or microcollapse), or because of variation in the structure of the dried cake, and thus of product resistance, or because of variations of the shelf temperature and of the pressure in the drying chamber, it should be evident that the shorter is the time interval between the test the better are the estimations that can be obtained.

### **Study of the influence of the duration of the PRT**

This section is focused on the investigation of the influence of the duration of the PRT on the results obtained using various model-based algorithms, namely MTM (in the formulation of Pikal et al.<sup>[10]</sup>), PRA and DPE. In order to assess the accuracy of the estimations provided by the various methods we will not use any experimental data: in fact, in case a thermocouple is used to measure product temperature, this can affect the dynamics of the product in that vial and the result can be not representative of the whole batch. Moreover, experimentally obtained values can be affected by radiation and by other sources of heterogeneity. Thus, mathematical simulation has been used to calculate the curves of pressure rise: by this way it is possible to compare the exact values of product temperature, of sublimation flow, and of the heat transfer coefficient, with the values estimated by means of the PRT-based algorithms. According to the previous discussion about the mathematical models that can be used to simulate the dynamics of the product during a freeze-drying process, the detailed model of Velardi and Barresi<sup>[37]</sup> has been used in this study. As in the previous section, the case study that has been considered is the freeze drying of a 10% by weight sucrose solution in tubing vials having a diameter of  $14.25 \cdot 10^{-3}$  m: the product thickness after freezing is  $7.21 \cdot 10^{-3}$  m, and the structure of the dried matrix is considered uniform. The primary drying is carried out at 10 Pa and using a shelf temperature of  $-20^\circ\text{C}$ . The batch is composed by 200 vials placed in

a chamber of  $0.2 \text{ m}^3$ ; the presence of inert gas, e.g. nitrogen, in the drying chamber has been assumed to be negligible during the entire cycle. The vials are considered to be perfectly shielded, i.e. radiation from the chamber walls and from the shelves does not affect the evolution of the product. The role of the heat capacity of the glass wall has been neglected. The last two assumptions are motivated by the fact that the goal of this study is to assess the impact of the duration of the PRT on the estimations obtained: to this purpose we removed any possible source of inaccuracy due to physical processes that are not taken into account by the models used to describe the PRT.

Figure 4 compares the results obtained using the algorithms MTM, PRA and DPE when the duration of the PRT is 30 s. Not only the product temperatures at the bottom of the vial and at the interface of sublimation are compared, but also the sublimation flow, that is required to estimate the progress of the primary drying, and the heat transfer coefficient  $K_v$ , that can be required by model-based control algorithms. The time evolution of the product temperature exhibits spikes in correspondence of the PRT: it is possible to see that the temperature increase due to the test can be important, for this test duration, when primary drying is approaching the end. Similarly, the spikes in the time evolution of the sublimation flow are due to the PRT: in fact, when the valve in the spool is opened at the end of the PRT, the pressure in the drying chamber is suddenly decreased, and this causes the increase of the sublimation flow, but in a very limited time interval (less than 1 minute) and, thus, it does not affect the drying time. The data of pressure rise are collected using a frequency of 10 Hz: higher frequencies increase the time required by the calculations, without improving the accuracy of the estimations, while lower frequencies (e.g. 1 Hz) can seriously impair the quality of the results. As it has been discussed in the previous section, this is related to the time constant of the process: in the case study the time constant is equal to 2-3 s at the beginning of the primary drying, and then it increases up to 5-6 s when approaching the end. When using a constant sampling frequency for all the cycle, this value should be at least of 5 Hz. Thus, 10 Hz can be a good compromise between accuracy and time required by the algorithms used to fit the experimental data. The time interval between two tests has been considered equal to 30 minutes: in this case study the shelf temperature is assumed to remain constant, and product resistance is assumed to vary linearly with the thickness of the dried layer (i.e. the diffusivity coefficient  $k_1$  is assumed to remain constant during the primary drying) as a consequence of the assumption of uniform matrix structure.

Results given in Figures 4 show that in all cases the product temperature estimated in the first part of the drying is accurate, but it becomes lower than the true value when the



system approaches the end of the primary drying. This is a well known behavior of all PRT-based algorithms that was motivated, in previous works, by taking into account batch heterogeneity: when the primary drying is approaching the end, sublimation is already finished in a fraction of vials (mainly the edge-vials, because of radiation from the chamber walls), while these algorithms continue interpreting pressure rise curves assuming batch uniformity, i.e. a constant number of sublimating vials. A decrease in pressure rise, corresponding to a lower sublimation rate, may thus be interpreted as a reduction of the front temperature. Our analysis evidences that this trend in the estimation of the product temperature can be obtained also in case of homogeneous batches, as in the case study the curves of pressure rise are obtained by simulating the evolution of a homogeneous batch. As it will be discussed in the following sections, batch heterogeneity is surely responsible, at least partly, for the observed behavior, but this can be also due to the optimization algorithm and caused by problem of ill-conditioning.

With respect to the sublimation flow, and, thus, to the frozen layer thickness, and to the heat transfer coefficient  $K_v$ , the estimations obtained by means of PRA and DPE algorithms are very similar and more accurate than those obtained by means of MTM: errors occur in the first and in the last part of the drying. The sublimation flow estimated by the MTM algorithm results to be lower than the correct value in the tested case: as a consequence, the time required to complete the main drying is overestimated.

Figure 5 shows the results obtained using the DPE algorithm for different durations of the PRT, namely 30 s, 10 s and 5 s, using the same sampling frequency. The accuracy of the estimations in the second part of the primary drying is significantly increased when the duration of the test is decreased. A similar trend is observed when PRA and MTM algorithms are used, with an improvement of the quality of predictions at lower acquisition time, even if it must be noted that when the duration of the test is 5 s the estimations obtained using the MTM are reliable only in the first half of the primary drying.

The rule of thumb that can be derived from this study is that the optimal duration of the PRT is close to the time constant of the process ( $\tau$ ) previously calculated (eq. (10)). In fact, if the duration of the PRT is lower than  $\tau$ , then it is not possible to "capture" the complete dynamics of the process. Besides, it must be considered that very low values can be not feasible from a practical point of view. The fact that it is sufficient to use the first part of the curve of pressure rise to get a reliable estimation of the parameters can be supported by the following analysis. The simple eq. (7) describing pressure rise during the PRT can be solved analytically, thus resulting in:

$$p_c = p_{c,0}e^{-t/\tau} + p_{w,i}\left(1 - e^{-t/\tau}\right) \quad (11)$$

In the time interval between the beginning of the PRT and when  $t = \tau$  the value of  $p_c$  varies between  $p_{c,0}$  and a value that is about 63% of the asymptotic value, that is equal to  $p_{w,i}$  according to the simplified model used for this analysis. If eq. (11) is substituted in eq. (5) we obtain:

$$\min_{p_{w,i}, k_1} \sum_k \left[ p_{c,0}e^{-t_k/\tau} + p_{w,i}\left(1 - e^{-t_k/\tau}\right) - p_{c,meas,k} \right]^2 \quad (12)$$

Then, for  $t > \tau$  both the value of the exponential functions and the difference between the measured pressure ( $p_{c,meas,k}$ ) and the pressure at the sublimating interface ( $p_{w,i}$ ) become small with respect to the values obtained at the beginning of the test. This means that in the error function that we are minimizing, after a time interval equal to  $\tau$  we add terms that can be neglected with respect to the first ones. As a consequence, a short duration of the PRT can be sufficient to get accurate estimations. In case the duration of the PRT is higher than  $\tau$ , the estimations become less accurate, in particular in the final part of the primary drying. As it will be discussed in the following paragraph, this can be a consequence of the ill-conditioning of the problem.

Besides, the use of short time intervals for the PRT is advisable also from the point of view of the preservation of the quality of the product, as during the PRT product temperature increases as the heating is not stopped. For this reason, the higher is the duration of the test, the higher is the temperature increase, as it can be seen in Figure 4 where the temperature profiles obtained for various duration of the test are compared and the spikes, corresponding to the temperature rise during the PRT, are higher when the duration of the test is increased. Nevertheless, slightly longer time intervals than the minimum calculated in the test case should be used when monitoring a real process because of two reasons:

- 1) the smaller is the duration of the PRT, the lower is the pressure increase, thus requiring pressure gauges with high resolution;
- 2) when dealing with real equipment, few seconds can be required to close the valve, thus affecting the first part of the curve of pressure rise.

### Ill-conditioning of the problem

When solving a nonlinear least-square optimization (eq. (5)) problem ill-conditioning has to be taken into account. In fact, frequently the observable signals are not rich enough to allow for accurate estimation of all the model parameters. This leads to an ill-conditioned estimation problem in which the parameter estimates become very sensitive to the data. To overcome the ill-conditioning it is possible to reduce problem dimensionality, i.e. the number of parameters that are estimated, by identifying those well-conditioned parameters that have strongly independent effects on the model output, and thus can be estimated robustly. The reliability of the estimations is significantly improved if only the well-conditioned parameters are estimated, while the ill-conditioned ones are fixed *a priori* using, for example, physical considerations about the process.<sup>[44]</sup> To illustrate the problem of ill-conditioning, we follow the reasoning presented by Burth and co-workers.<sup>[44]</sup> Let  $\theta$  be the vector of the parameters that are estimated (i.e.  $p_{w,i}$  and  $k_1$ ), and

$$r(\theta) = p_c(\theta) - p_{c,meas} \quad (13)$$

denote the residual error. The Jacobian (or gradient) matrix of the error vector with respect to the parameters vector can be calculated:

$$J_{i,j} = \frac{\partial r_i(\theta)}{\partial \theta_j} \quad (14)$$

It is possible to demonstrate that if  $J$  is singular the model parameters are not uniquely determinable from the available observation data: such an estimation problem is said to be over-parameterized (see Bard<sup>[45]</sup> for a more detailed analysis). Typically,  $J$  is not exactly singular, but nearly so, with its largest singular value much greater than its smallest. Nearness to singularity is measured by the condition number,  $\kappa(J)$ , which is given by the ratio of the largest to the smallest eigenvalue. This nearness to singularity gives an ill-conditioned problem, in which small numerical errors or noise in the data can radically modify the solution. To overcome the problem of ill-conditioning, one (or more) parameters should be discarded from the estimation formulation. Care must be paid when reducing the dimensionality of the model, i.e. the number of parameters, as over-simplification can occur, thus resulting in inaccurate results. This issue will be discussed in the following paragraph, where a new approach for interpreting the PRT will be presented.

Let us analyze ill-conditioning of the methods based on the PRT. To this purpose, we use the simple model given by eq. (12). It is possible to calculate the Jacobian matrix and the

condition number, that is a function of product temperature (through  $p_{w,i}$ ) and of product resistance to vapor flow (through  $\tau$ ). Figure 6 shows the result of this calculation for two different durations of the PRT, namely 5 and 30 s: it has to be remarked that the higher is the duration of the test, the higher is the condition number, thus motivating the results given in the previous section about the optimal selection of the duration of the test. Besides, when product resistance increases, the condition number increases and, as said before, a high value of  $\kappa$  means ill-conditioned problem. The trajectory of the system for the case study is shown in the contour plots shown in the right side of Figure 6 (curves A). A different trajectory of the system is shown in case the shelf temperature is manipulated in order to maintain the interface temperature equal to  $-40^{\circ}\text{C}$  (curves B). The control system proposed by Fissore et al.<sup>[46]</sup> has been used to this purpose. It is possible to observe that during primary drying the resistance of the product to vapor flow increases, due to the increase of the thickness of the dried layer, and, thus, a lower accuracy of the estimations obtained is expected when the drying is approaching the end. Moreover, also in case product resistance to vapor flow is high, i.e. when the sublimation flow is low, the accuracy of the results obtained by means of the various algorithms is also expected to be poor.

Results shown in Figure 6 demonstrate that the estimation problem can become ill-conditioned in the second part of the primary drying. One of the suggestions that can be found in the Literature when dealing with ill-conditioned problems is to reduce the number of samples that are used to solve the minimization problem: this can motivate the results shown in the previous paragraph, where the accuracy of the estimations in the second part of the drying was improved by reducing the duration of the test from 30 s to 5 s.

Finally, it has to be remarked that it is not possible to define a threshold value for the condition number, and, thus, to state that the problem is ill-conditioned when  $\kappa$  is higher than this value. Nevertheless, this analysis gives two important results:

- i) when drying approaches the end, condition number of the problem increases and, thus, the accuracy of the estimation is expected to be worsen;
- ii) when the duration of the PRT is reduced, the condition number decreases and, thus, the accuracy of the estimation is expected to be improved.

## DPE<sup>+</sup> algorithm

According to the conclusions of the previous sections, we propose a modification of the DPE algorithm of Velardi et al.<sup>[18]</sup> in order to improve problem conditioning, and, thus, the accuracy of the estimations. The basic idea is to calculate product resistance from the slope of the curve of pressure rise at the beginning of the test, and to estimate only the interface temperature through the least-square minimization. In fact, once the pressure rise curve has been acquired, and, eventually, filtered to reduce the noise of the experimental measurements, the sublimation rate, at a certain time during the test, can be calculated without using any model, but only evaluating the slope of the curve of pressure rise:

$$J_w = \frac{V_c M_w}{N_v A_p R T_c} \frac{dp_{w,c}}{dt} \quad (15)$$

Several methods can be used to numerically evaluate the first derivative of a curve; in the work here presented a natural cubic spline has been used to fit the experimental data (even in the case these data are obtained by means of mathematical simulation of the process), and the first derivative of the interpolated function has been approximated with the first derivative, taken at the knots, of the spline. Once the value of  $\frac{dp_{w,c}}{dt}$  has been calculated, the flow rate of the water vapor can be estimated, provided that the value of  $T_c$  is known.

The sublimation rate  $J_w$  can be expressed as a function of the ice front temperature and of the resistance to the mass transfer of vapor flow through the solid matrix as shown in the following:

$$J_w = \left( \frac{1}{R_p + R_s} \right) (p_{w,i}(T_i) - p_{w,c}) \quad (16)$$

The key variable to be monitored is the temperature of the moving front at the beginning of the test, thus the previous equation is written at  $t = t_0$ . Combining eq. (15) and (16), the mass transfer resistance can be written as a function of  $T_c$  and of the initial slope of the pressure rise curve as follows:

$$R_{ps} = (R_p + R_s) = \frac{N_v A_p R T_c}{V_c M_w} \left( \frac{dp_{w,c}}{dt} \right)_{t=t_0}^{-1} (p_{w,i}(T_i)|_{t=t_0} - p_{w,c,0}) \quad (17)$$

It seems convenient to express the flow rate in eq. (17) in terms of  $(R_p + R_s)$ , instead of  $k_1$  and  $L_f$ : thus, the mass transfer coefficient can be calculated even if the thickness of the frozen layer is not known *a priori*. This allows avoiding the loop required to determine a consistent

value of  $L_f$ . Moreover,  $(R_p + R_s)$  is the total resistance to the vapor flow through the dried layer, the stopper, and the drying chamber, while the parameter  $k_1$  may locally change and, therefore, the previous DPE algorithm can only estimate an average value of the effective diffusivity. In any case, considering that:

$$\frac{1}{R_p} = \frac{k_1 M_w}{RT_i (L - L_f)} \quad (18)$$

it is straightforward to pass from one notation to the other ( $R_s$  can be determined experimentally).

It is clear that once a pressure rise curve has been acquired, and its first derivative at  $t = t_0$  has been calculated, the value of  $R_p$  depends only on  $T_{c,0}$  that, in turn, is a function of  $T_{i,0}$ . Conversely, if the ice front temperature has been somehow estimated, the value of  $R_p$  is known; thus, unlike the previous approach, the parameter of the model to be estimated for the interpretation of pressure rise curve is only  $T_{i,0}$ .

Chamber temperature is required to calculate  $R_{ps}$  using eq. (17). Such temperature can be hardly measured, and significant temperature gradients exist in the chamber: in fact, the temperature of the vapor near the wall and the surface of the shelves is higher than that of the vapor near the sublimating interface. All the PRT base algorithms require knowing the value of  $T_c$ , and assumed either  $T_c = T_i$  or  $T_c = T_s$ . Chamber temperature can be assumed equal to the mean value of  $T_i$  and  $T_s$  (see eq. (8)), i.e.  $T_c = T_i(1 + \zeta)$  and, being  $\zeta \ll 1$ , then, for simplicity, we can assume that  $T_c$  is equal to the temperature of the product at the moving front position, i.e.  $T_{c,0} = T_{i,0}$ . This hypothesis is generally acceptable as the error in the estimation of  $T_c$  is about 5-7% (if  $T_c = 0^\circ\text{C}$  and  $T_i = -30^\circ\text{C}$  the error in the value of  $T_c$  due to this hypothesis is 6%) and the error in the estimation of  $R_{ps}$  is of the same order of magnitude. Anyway, if the shelf temperature is available, the average value can be used.

The equations of the DPE<sup>+</sup> algorithm are those of the DPE algorithm (see Appendix 3), writing the mass balance equation in the drying chamber in terms of  $R_p$ :

$$\frac{V_c M_w}{RT_c} \frac{dp_{w,c}}{dt} = N_v A_p \frac{1}{R_{ps}} (p_{w,i} - p_{w,c}) \quad (19)$$

and calculating the heat transfer coefficient  $K_v$  as:

$$K_v = \left[ \frac{T_s - T_{i,0}}{\frac{\Delta H_s}{R_{ps}} (p_{w,i,0} - p_{w,c,0})} - \frac{L_f}{\lambda_f} \right]^{-1} \quad (20)$$

Therefore, the steps of the optimization procedure are the following:

1. Initial guess of  $T_{i,0}$ .
2. Calculation of the first derivative of the pressure rise curve at  $t = t_0$  and of  $R_{ps}$  using eq. (17).
3. Determination of  $L_f$  from eq. (46), using the values measured and computed in the pressure rise test run at time  $t = t_0^{(-1)}$ .
4. Determination of  $K_v$  from eq. (20).
5. Determination of the initial temperature profile in the frozen mass, from eq. (37).
6. Integration of model equations describing pressure rise in the time interval  $(t_0, t_f)$ , where  $t_f - t_0$  is the time length of the PRT, in order to calculate  $p_{c,k}$ .
7. Evaluation of  $T_{i,0}$  that best fits the simulated chamber pressure to the measured data.

Using the proposed approach only product temperature at the interface of sublimation is estimated, instead of two parameters (e.g. product temperature and dried layer resistance to mass flow). This means that problem dimension is reduced, thus providing a solution to problem ill-conditioning, as it has been discussed in the previous section. It has to be remarked that the model used by DPE<sup>+</sup> algorithm to describe pressure rise during the PRT is exactly the same of DPE algorithm, i.e. no simplifications are introduced. The main difference of DPE<sup>+</sup> algorithm with respect to the original method is that it makes use of a further piece of information coming from the pressure rise measurement, i.e. that the slope of the curve of pressure rise is proportional to the sublimation flow and this allows to reduce the number of variables estimated by means of best-fit.

Figure 7 shows that the improved version of the DPE algorithm allows to obtain reliable estimations of  $T_i$  and of the frozen layer thickness throughout the primary drying; also the heat transfer coefficient  $K_v$  (not shown) is accurately estimated up to the end, and the end of the main drying is predicted reliably. In this case the duration of the PRT is 30 s, thus evidencing the correctness of our analysis: in fact, being lower the condition number, results are less affected by over-fitting. Calculations have been done also for lower duration of the PRT, giving almost the same results: thus, the proposed algorithm improves the robustness of the method, as the results are less sensitive to the duration of the test.

## Experimental results

Figure 8 shows an example of the estimations obtained by means of MTM (in the formulation of Pikal et al.<sup>[10]</sup>), PRA, DPE, and DPE<sup>+</sup> algorithms in case of a real process: the test has been carried out in a pilot-scale equipment (a modified *LyoBeta* 25, by Telstar) with a drying chamber volume of 0.2 m<sup>3</sup>; vials have been shielded to minimize radiation effects. The duration of the PRT is 30 s, according to the calculation of the time constant of the process, and the time interval between two tests is 30 min. While the original DPE algorithm estimates a (wrong) decreasing value for  $T_i$  after 8 h since the beginning of the primary drying, similarly to the results obtained in this case also by other PRT-based tools, the DPE<sup>+</sup> algorithm allows obtaining correct estimations up to 13 h since the beginning of the primary drying. In the experimental run the batch is not homogeneous, but this is not the only explanation of the decrease of interface temperature estimated, as it has been previously explained, and, thus results are significantly improved using the DPE<sup>+</sup> algorithm. The values of  $T_i$  estimated using the DPE<sup>+</sup> algorithm start decreasing only when the ratio of the pressure signals given by a capacitive gauge (Baratron) and by a Pirani sensor, generally used to assess the end of the primary drying, decreases. With respect to the estimation of the sublimation flow and of the heat transfer coefficient  $K_v$ , the values obtained by means of PRA, DPE, and DPE<sup>+</sup> algorithms are very close, while MTM always estimates lower values, similarly to what was observed when mathematical simulation was used to calculate the curves of pressure rise.

## Conclusions

When solving a nonlinear least-square optimization problem to retrieve the status of a system, or the values of some parameters, there are various issues that have to be taken into account in order to get reliable results, i.e. the sampling frequency, the duration of the test, the time interval between two tests, the ill-conditioning of the problem, and the mathematical model that is used to interpret the experimental measurements. All these issues have to be taken into account when using the Pressure Rise Test to monitor the primary drying of a lyophilization process: the effects of various model assumptions (i.e. the effect of vial wall, and of radiation) have been discussed, and general guidelines to improve the results have been given.

Comparison of various approaches previously proposed in Literature has shown that the interface temperature can be generally estimated reliably, independently from the algorithm used, in the first part of the drying, but differences become significant toward the end of the



primary drying, and when sublimation flow or position of the sublimating interface is considered.

Ill-conditioning of the problem has been investigated, evidencing that the parameters estimates can become very sensitive to the data, depending on process conditions and product characteristics. To overcome the ill-conditioning, the number of parameters that are estimated has to be reduced. This analysis is at the basis of the  $DPE^+$  algorithm, whose effectiveness is demonstrated by means of mathematical simulations and experimental runs. This algorithm is demonstrated to be very robust, as the duration of the test does not affect significantly the estimates; in any case, a short duration of the PRT is advisable in order to reduce product temperature increase due to the test.

Besides, there is still an open issue concerning the use of the PRT for freeze-drying monitoring, i.e. the heterogeneity of the batch. It would be very important to get estimates not only of mean values of product temperature and of residual ice content, but also of the variance of both variables among the vials of the batch. This problem will be investigated in a future paper.

### **Acknowledgement**

The authors would like to acknowledge Dr. Salvatore Velardi (Politecnico di Torino, Italy) for the valuable contribution in the realization of the software used for the mathematical simulation of the process.

## References

1. Franks, F. Freeze-drying of Pharmaceuticals and Biopharmaceuticals; Royal Society of Chemistry; Cambridge, 2007.
2. Pikal, M.J.; Shah, S. The collapse temperature in freeze drying: dependence on measurement methodology and rate of water removal from the glassy phase, *International Journal of Pharmaceutics* **1990**, *62* (2-3), 165–186.
3. Wang, W. Lyophilization and development of solid protein pharmaceuticals. *International Journal of Pharmaceutics* **2000**, *203* (1-2), 1–60.
4. Rambhatla, S.; Obert, J.P.; Luthra, S.; Bhugra, C.; Pikal, M.J. Cake shrinkage during freeze drying: a combined experimental and theoretical study. *Pharmaceutical Development and Technology* **2005**, *10* (1), 33–40.
5. Hsu, C.C.; Ward, C.A.; Pearlman, R.; Nguyen, H.M.; Yeung, D.A., Curley, J.G. Determining the optimum residual moisture in lyophilized protein pharmaceuticals. *Developments in Biological Standardization* **1992**, *74*, 255-271.
6. Wiggenghorn, M.; Presser, I.; Winter, G. The current state of PAT in freeze-drying. *American Pharmaceutical Review* **2005**, *8*, 38-44; *European Pharmaceutical Review* **2005**, *10*, 87-92.
7. Barresi, A.A.; Fissore, D.; Product quality control in freeze drying of pharmaceuticals. In *Modern drying technology - Volume 3*; Tsotsas, E., Mujumdar A.S., Eds.; Wiley-VCH: Weinheim, In press.
8. Barresi, A.A.; Pisano, R.; Fissore, D.; Rasetto, V.; Velardi, S.A.; Vallan, A.; Parvis, M.; Galan, M. Monitoring of the primary drying of a lyophilization process in vials. *Chemical Engineering & Processing* **2009**, *48* (1), 408-423.
9. Neumann, K.H. Freeze-drying apparatus. United States Patent No. 2994132, 1961.
10. Pikal, M.J.; Tang, X.; Nail, S.L. Automated process control using manometric temperature measurement. United States Patent No. 6971187 B1, 2005.
11. Tang, X.C.; Nail, S.L.; Pikal, M.J. Freeze-drying process design by manometric temperature measurement: design of a smart freeze-dryer. *Pharmaceutical Research* **2005**, *22* (4), 685-700.
12. Fissore, D.; Barresi, A.A.; Pisano, R. Method for monitoring the secondary drying in a freeze-drying process. European Patent Application No. 08013243.4-1266, 2008.
13. Milton, N.; Pikal, M.J.; Roy, M.L.; Nail, S.L. Evaluation of manometric temperature measurement as a method of monitoring product temperature during lyophilization. *PDA*

- Journal of Pharmaceutical Science & Technology **1997**, 51 (1), 7-16.
14. Tang, X.C.; Nail, S.L.; Pikal, M.J. Evaluation of manometric temperature measurement, a Process Analytical Technology tool for freeze-drying: part I, product temperature measurement. AAPS Pharmaceutical Science and Technology **2006**, 7 (1), article 14, 9 pp.
  15. Tang, X.C.; Nail, S.L.; Pikal, M.J. Evaluation of manometric temperature measurement, a Process Analytical Technology tool for freeze-drying: part II, measurement of dry layer resistance. AAPS Pharmaceutical Science and Technology **2006**, 7 (4), article 93, 8 pp.
  16. Tang, X.C.; Nail, S.L.; Pikal, M.J. Evaluation of manometric temperature measurement (MTM), a Process Analytical Technology tool in freeze drying, part III: heat and mass transfer measurement. AAPS Pharmaceutical Science and Technology **2006**, 7 (4), article 97, 7 pp.
  17. Chouvenec, P.; Vessot, S.; Andrieu, J.; Vacus, P. Optimization of the freeze-drying cycle: a new model for pressure rise analysis. Drying Technology **2004**, 22 (7), 1577-1601.
  18. Velardi, S.A.; Rasetto, V.; Barresi, A.A. Dynamic Parameters Estimation Method: advanced Manometric Temperature Measurement approach for freeze-drying monitoring of pharmaceutical. Industrial & Engineering Chemistry Research **2008**, 47 (21), 8445-8457.
  19. Velardi, S.A.; Barresi, A.A. Method and system for controlling a freeze drying process. International application No. PCT/EP2007/059921 (19/09/2007). International Publication No. WO 2008/034855 A2 (27 March 2008, World Intellectual Property Organization [Priority EP 06019587.2 200619587 (19/09/2006)]).
  20. Barresi, A.A.; Velardi, S.A.; Pisano, R.; Rasetto, V.; Vallan, A.; Galan, M. In-line control of the lyophilization process. A gentle PAT approach using software sensors. International Journal of Refrigeration **2009**, 32 (5), 1003-1014.
  21. Neumann, K.H. Determining temperature of ice. In Freeze-drying of Foods and Biologicals; Noyes, R. Ed.; Noyes Development Corporation: Park Ridge, 1968.
  22. Nail, S.L.; Johnson, W. Methodology for in-process determination of residual water in freeze-dried products. Developments in Biological Standardization **1991**, 74, 137-151.
  23. Willemer, H. Measurement of temperature, ice evaporation rates and residual moisture contents in freeze-drying. Development of Biological Standardization **1991**, 74, 123-136.
  24. Oetjen, G.W. Freeze-Drying. Wiley-VCH; Weinheim, 1999.
  25. Oetjen, G.W.; Haseley, P.; Klutsch, H.; Leineweber, M. Method for controlling a Freeze-Drying process. United States Patent No. 6163979, 2000.

26. Oetjen, G.W.; Haseley, P. Freeze-Drying (2nd edition). Wiley-VHC; Weinheim, 2004.
27. Liapis, A.I.; Sadikoglu, H. Dynamic pressure rise in the drying chamber as a remote sensing method for monitoring the temperature of the product during the primary drying stage of freeze-drying. *Drying Technology* **1998**, *16* (6), 1153-1171.
28. Obert, J.P. Modélisation, optimisation et suivi en ligne du procédé de lyophilisation. Application à l'amélioration de la productivité et de la qualité de bactéries lactiques lyophilisées. PhD Thesis, INRA Paris-Grignon, 2001.
29. Sadikoglu, H.; Liapis A.I. Mathematical modelling of the primary and secondary stages of bulk solution freeze-drying in trays: parameter estimation and model discrimination by comparison of theoretical results with experimental data. *Drying Technology* **1997**, *15* (3-4), 43-72.
30. Sheehan, P.; Liapis, A.I. Modeling of the primary and secondary drying stages of the freeze drying of pharmaceutical products in vials: numerical results obtained from the solution of a dynamic and spatially multidimensional lyophilization model for different operational policies. *Biotechnology and Bioengineering* **1998**, *60* (6), 712–728.
31. Pikal, M.J. Use of laboratory data in freeze-drying process design: heat and mass transfer coefficients and the computer simulation of freeze-drying. *Journal of Parenteral Science and Technology* **1985**, *39* (3), 115–139.
32. Hottot, A.; Peczalski, R.; Vessot, S.; Andrieu, J. Freeze-drying of pharmaceutical proteins in vials: modeling of freezing and sublimation steps. *Drying Technology* **2006**, *24* (5), 561-570.
33. Brülls, M.; Rasmuson, A. Ice sublimation in vial lyophilization. *Drying Technology* **2009**, *27* (5), 695-706.
34. Millman, M.J.; Liapis, A.I.; Marchello, J.M. An analysis of the lyophilisation process using a sorption sublimation model and various operational policies, *AIChE Journal* **1985**, *31* (10), 1594-1604.
35. Ybema, H.; Kolkman-Roodbeen, L.; te Booy, M.P.W.M.; Vromans, H. Vial lyophilization: calculations on rate limiting during primary drying. *Pharmaceutical Research* **1995**, *12* (9), 1260–1263.
36. Brülls, M.; Rasmuson, A. Heat transfer in vial lyophilization. *International Journal of Pharmaceutics* **2002**, *246* (1), 1-16.
37. Velardi, S.A.; Barresi, A.A. Development of simplified models for the freeze-drying process and investigation of the optimal operating conditions. *Chemical Engineering Research & Design* **2008**, *86* (1), 9-22.

38. Barresi, A.A.; Pisano, R.; Rasetto, V.; Fissore, D.; Marchisio, D.L. Model-based monitoring and control of industrial freeze-drying processes: effect of batch non-uniformity. *Drying Technology*. In press.
39. Goff, J.A.; Gratch, S. Low-pressure properties of water from -160 to 212 F. *Transactions of the American Society of Heating and Ventilating Engineers* **1946**, 95-122. Presented at the 52nd Annual Meeting of the American Society of Heating and Ventilating Engineers, New York, 1946.
40. Vömel H. Saturation vapor pressure formulations.  
<http://cires.colorado.edu/~voemel/vp.html>
41. Wanger, W.; Saul, A.; Pruss, A. International equations for the pressure along the melting and along the sublimation curve of ordinary water substance. *Journal of Physical and Chemical Reference Data* **1994**, 23, 515-525.
42. Galan, M.; Velardi, S.A.; Pisano, R.; Rasetto, V.; Barresi, A.A. A gentle PAT approach to in-line control of the lyophilization process. *Proceedings of New ventures in Freeze-Drying Conference*, Strasbourg, France, November 7-9, 2007. *Refrigeration Science and Technology Proceedings No 2007-3*; CD-ROM Edition, Institut International du Froid, Paris, 17 pp.
43. Schelenz, G.; Engel, J.; Rupprecht, H. Sublimation drying lyophilization detected by temperature profile and X-ray technique. *International Journal of Pharmaceutics* **1994**, 113 (2), 133-140.
44. Burth, M.; Verghese, G.; Vélez-Reyes, M. Subset selection for improved parameter estimation in on-line identification of a synchronous generator. *IEEE Transactions on Power Systems* **1999**, 14 (1), 218–225.
45. Bard, Y. *Nonlinear Parameter Estimation*; Academic Press; New York, 1974.
46. Fissore, D.; Velardi, S.A.; Barresi, A.A. In-line control of a freeze-drying process in vials. *Drying Technology* **2008**, 26 (6), 685-694.
47. Rambhatla, S.; Ramot, R.; Bhugra, C.; Pikal, M.J. Heat and mass transfer scale-up issues during freeze drying: II. Control and characterization of the degree of supercooling. *AAPS Pharmaceutical Science and Technology* **2004**, 5 (4), article 58, 9 pp.
48. Hottot, A.; Vessot, S.; Andrieu, J. Determination of mass and heat transfer parameters during freeze-drying cycles of pharmaceuticals products. *PDA Journal of Pharmaceutical Science Technology* **2005**, 59 (2), 138-153.

## List of symbols

$A_p$	cross surface of the product in the vial, $\text{m}^2$
$A_v$	bottom surface of the vial, $\text{m}^2$
$c_{p,f}$	specific heat of the frozen layer, $\text{J kg}^{-1}\text{K}^{-1}$
$c_{p,v}$	specific heat of the glass, $\text{J kg}^{-1}\text{K}^{-1}$
$D_{\text{des}}$	desorption rate of the batch, $\text{Pa s}^{-1}$
$F_{\text{leak}}$	leakage rate, $\text{Pa s}^{-1}$
$\Delta H_{\text{des}}$	heat of desorption, $\text{J mol}^{-1}$
$\Delta H_s$	heat of sublimation, $\text{J mol}^{-1}$
$J$	Jacobian matrix of the error vector with respect to the parameters vector
$J_w$	sublimation flow, $\text{kg s}^{-1} \text{m}^{-2}$
$k_1$	effective diffusivity of water vapor in the dried layer, $\text{m}^2 \text{s}^{-1}$
$L$	product thickness after freezing, $\text{m}$
$L_f$	thickness of the frozen product, $\text{m}$
$L_v$	height of the vial in contact with the product, $\text{m}$
$K$	parameter of the MTM algorithm, $\text{s}^{-1}$
$K_v$	heat transfer coefficient between the bottom of the vial and the shelf, $\text{J s}^{-1}\text{m}^{-2}\text{K}^{-1}$
$M_w$	molar mass of water, $\text{kg mol}^{-1}$
$m$	mass of product in a vial, $\text{g}$
$m_v$	mass of the vial, $\text{kg}$
$N_v$	number of vials of the batch
$p_c$	total pressure in the drying chamber, $\text{Pa}$
$p_{\text{in},c}$	partial pressure of the inert gas in the chamber, $\text{Pa}$
$p_{w,i}$	vapor pressure at the sublimation interface, $\text{Pa}$
$p_{w,c}$	water partial pressure in the drying chamber, $\text{Pa}$
$R$	ideal gas constant, $\text{J K}^{-1}\text{mol}^{-1}$
$R_p$	mass transfer resistance to vapor flow in the dried layer, $\text{m s}^{-1}$
$\hat{R}_p$	mass transfer resistance to vapor flow in the dried layer, $\text{cm}^2 \text{Torr h g}^{-1}$ .
$R_{ps}$	mass transfer resistance to vapor flow in the dried layer and in the stopper, $\text{m s}^{-1}$
$R_s$	mass transfer resistance to vapor flow in the stopper, $\text{m s}^{-1}$
$\hat{R}_s$	mass transfer resistance to vapor flow in the stopper, $\text{cm}^2 \text{Torr h g}^{-1}$ .
$r$	residual error, $\text{Pa}$

$T_b$	product temperature at the bottom of the vial, K
$T_i$	product temperature at the sublimation interface, K
$\Delta T_i$	temperature difference across the frozen layer, K
$T$	temperature, K
$T_s$	shelf temperature, K
$T_c$	temperature of the vapor in the drying chamber, K
$t$	time, s
$V_c$	chamber volume, m <sup>3</sup>
$X$	parameter of the MTM algorithm, Torr s <sup>-1</sup>
$z$	axial coordinate, m

### *Subscripts*

0	at the beginning of the PRT
(-1)	PRT before the actual one
<i>eff</i>	effective value
<i>f</i>	at the end of the PRT
<i>meas</i>	measured value

### *Greeks*

$\alpha$	portion of the mass of a vial in contact with the product
$\zeta$	parameter used to express $T_c$ as a function of $T_i$
$\theta$	vector of parameters that are estimated using the PRT
$\kappa$	condition number
$\lambda_f$	thermal conductivity of the frozen layer, J s <sup>-1</sup> m <sup>-1</sup> K <sup>-1</sup>
$\lambda_v$	thermal conductivity of the glass, J s <sup>-1</sup> m <sup>-1</sup> K <sup>-1</sup>
$\rho_d$	density of the dried layer, kg m <sup>-3</sup>
$\rho_f$	density of the frozen layer, kg m <sup>-3</sup>
$\tau$	time constant of the process, s

### *Abbreviations*

DPE	Dynamic Parameters Estimation
MTM	Manometric Temperature Measurement
PRA	Pressure Rise Analysis

PRT      Pressure Rise Test



## Appendix 1. The *Manometric Temperature Measurement* algorithm.

The MTM algorithm<sup>[13]</sup> assumes that the pressure response during the PRT is described by the following equation:

$$p_c(t) = p_{w,i} - (p_{w,i} - p_{w,c,0})e^{-Kt} + \frac{p_{w,i}\Delta H_s}{RT_i^2} \frac{\Delta T_i}{2} \left( 1 - \frac{8}{\pi^2} e^{-\frac{\lambda_f \pi^2}{\rho_f c_{p,f} L_f} t} \right) + \left[ \frac{p_{w,i}\Delta H_s}{RT_i^2} \frac{1}{c_{p,f} L_f \rho_f} K_v (T_s - T_b) \right] t + F_{\text{leak}} t \quad (21)$$

where:

$$T_b = T_i + \Delta T_i \quad (22)$$

$$K = \frac{N_v A_p R T_c}{M_w V_c R_p} \quad (23)$$

The temperature difference across the frozen layer  $\Delta T_i$  is assumed to be constant and equal to 2°C and  $T_c$ , the temperature of the vapor in the drying chamber, is assumed to be equal to  $T_s$ . A slightly different equation is given by Pikal et al.<sup>[10]</sup> and by Tang et al.<sup>[14],[15],[16]</sup>. In this case the pressure evolution during the PRT is given by:

$$p_c(t) = p_{w,i} - (p_{w,i} - p_{w,c,0})e^{-\left(\frac{3.461 N_v A_p T_s}{3600 V_c (\hat{R}_p + \hat{R}_s)}\right)t} + 0.0465 p_{w,i} \Delta T_i \left( 1 - 0.811 e^{\frac{0.114}{L_f} t} \right) + X t \quad (24)$$

where  $X$  is a fitting parameter and  $\Delta T_i$  is assumed constant and equal to 2°C, but the following equation is also given for the calculation of  $\Delta T_i$ :

$$\Delta T_i = \frac{24.7 L_f \frac{p_{w,i} - p_{w,c,0}}{\hat{R}_p + \hat{R}_s} - 0.0102 L_f (T_s - T_i)}{1 - 0.0102 L_f} \quad (25)$$

In eq. (24) and (25)  $p_{w,i}$  and  $p_{w,c}$  are measured in Torr,  $A_p$  in cm<sup>2</sup>,  $V_c$  in liter and  $L_f$  in cm. Rambhatla et al.<sup>[47]</sup> assumed  $\Delta T_i = 1^\circ\text{C}$  and they noticed no difference in the values of  $R_p$  and  $p_{w,i}$  with respect to those obtained using eq. (25). The ice sublimation rate per vial is calculated by :

$$\frac{dm}{dt} = A_p \frac{p_{w,i} - p_{w,c}}{\hat{R}_p} \quad (26)$$

where  $p_{w,i}$  and  $p_{w,c}$  are measured in Torr, and  $A_p$  in cm<sup>2</sup>. Integration of eq. (26) allows to calculate the mass of ice sublimated at various time and, thus, the frozen layer thickness  $L_f$

required to solve eq. (24) and (25).

The heat transfer coefficient  $K_v$  is calculated by assuming that the heat flow from the shelf to the vials is equal to the heat consumed by ice sublimation:

$$K_v A_v (T_s - T_b) = \Delta H_s J_w \quad (27)$$

and, thus:

$$K_v = \frac{\Delta H_s J_w}{A_v (T_s - T_b)} \quad (28)$$

The contribution of the thermal inertia of the glass wall and of the desorption of the bound water is taken into account in the equation proposed by Obert<sup>[28]</sup>:

$$p_c(t) = p_{w,i} - (p_{w,i} - p_{w,c,0})e^{-Kt} + \frac{p_{w,i}\Delta H_s}{RT_i^2} \frac{\Delta T_i}{2} \left( 1 - \frac{8}{\pi^2} e^{-\frac{\lambda_f \pi^2}{\rho_f c_{p,f} L_f} t} \right) +$$

$$+ \left[ \frac{p_{w,i}\Delta H_s}{RT_i^2} \frac{1}{c_{p,f} L_f \rho_f + \frac{m_v c_{p,v}}{A_v}} K_v (T_s - T_b) \right] t + F_{\text{leak}} t + D_{\text{des}} t \quad (29)$$

Assuming that the heat flow from the shelf to the vials is equal to the heat consumed by ice sublimation, the heat transfer coefficient  $K_v$  appearing in eq. (29) is replaced by the following expression:

$$K_v = \frac{\Delta H_s (p_{w,i} - p_{w,c})}{R_p (T_s - T_b)} \quad (30)$$

## Appendix 2: The *Pressure Rise Analysis* algorithm.

The PRA algorithm<sup>[17]</sup> assumes that the rate of water vapor pressure increase during the PRT is given by:

$$\frac{dp_{w,c}}{dt} = \frac{N_v A_p R T_c}{M_w V_c R_p} (p_{w,i} - p_{w,c}) + D_{\text{des}} \quad (31)$$

The above equation is combined with a macroscopic heat balance for the frozen layer, under the assumption that the temperature increase at the interface,  $dT_i/dt$ , is the same as the mean product temperature rise:

$$\left( \rho_f c_{p,f} L_f + \frac{\alpha m_v c_{p,v}}{A_v} \right) \frac{dT_i}{dt} = K_v (T_s - T_b) - \frac{\Delta H_s}{R_p} (p_{w,i} - p_{w,c}) - \frac{M_w V_c \Delta H_{des}}{N_v A_p R T_c} D_{des} \quad (32)$$

In this case in the energy balance only a fraction of the thermal inertia of the vial is considered, corresponding, in principle, with "the fraction of vial in contact with the product"; actually,  $\alpha$  is a parameter to be estimated. The leak of the freeze drier chamber is assumed constant and given by  $F_{leak} = dp_{in}/dt$  and the total chamber pressure measured during the PRA is given by:

$$p_c(t) = p_{w,c}(t) + p_{in}(t) \quad (33)$$

The value of  $K_v$  is calculated from steady-state hypothesis, as well as the temperature of the vial bottom, assumed to remain constant during the PRT:

$$K_v (T_s - T_b) = \frac{\Delta H_s}{R_p} (p_{w,i,0} - p_{w,c,0}) + \frac{M_w V_c \Delta H_{des}}{N_v A_p R T_c} D_{des} \quad (34)$$

$$T_b = \left( \frac{L_v}{\lambda_v} + \frac{L_f}{\lambda_f} \right) \frac{\Delta H_s}{R_p} (p_{w,i,0} - p_{w,c,0}) + T_{i,0} \quad (35)$$

### Appendix 3: The Dynamic Parameters Estimation algorithm.

The DPE algorithm<sup>[18]</sup> describes the heat transfer and the local evolution of the temperature  $T=T(z)$  in the frozen layer during the PRT by means of the following equations:

$$\frac{\partial T}{\partial t} = \frac{\lambda_f}{\rho_f c_{p,f}} \frac{\partial^2 T}{\partial z^2} \quad \text{for } t > t_0, \quad 0 \leq z \leq L_f \quad (36)$$

$$T|_{t=0} = T_{i,0} + \frac{z}{\lambda_f} \Delta H_s \left[ \frac{(L - L_f) R T_{i,0}}{k_l M_w} + R_s \right]^{-1} (p_{w,i,0} - p_{w,c,0}) \quad \text{for } 0 \leq z \leq L_f \quad (37)$$

$$\lambda_f \frac{\partial T}{\partial z} \Big|_{z=0} = \Delta H_s \left[ \frac{(L - L_f) R T_{i,0}}{k_l M_w} + R_s \right]^{-1} (p_{w,i,0} - p_{w,c,0}) \quad \text{for } t \geq t_0 \quad (38)$$

$$\lambda_f \frac{\partial T}{\partial z} \Big|_{z=L_f} = K_v (T_s - T_b) \quad \text{for } t \geq t_0 \quad (39)$$

Thermodynamic equilibrium is assumed at the sublimating front, corresponding to the axial position  $z = 0$ . The heat fluxes at  $z = 0$  and at  $z = L_f$ , corresponding to the internal bottom of the vial, are generally not equal during the PRT, because of accumulation in the frozen layer,

except at the beginning because of the pseudo-stationary hypothesis. Thanks to this assumption, the expression for the heat transfer coefficient,  $K_v$ , assumed constant during the PRT, can be derived by equating the boundary conditions (38) and (39), both taken at  $t = t_0$ . Thus:

$$K_v = \left[ \frac{T_s - T_{i,0}}{\Delta H_s \left[ \frac{(L - L_f)RT_{i,0}}{k_1 M_w} + R_s \right]^{-1} - \frac{L_f}{\lambda_f}} \right]^{-1} \quad (40)$$

The previous equations are completed with the equation providing the dynamics of the water vapor pressure rise in the chamber, which consists in the material balance for the vapor flowing into the chamber environment. Applying the ideal gas law and rewriting the mass flow rates as functions of the pressure driving force between the interface and the chamber, it follows:

$$\left( \frac{M_w V_c}{RT_c} \right) \frac{dp_{w,c}}{dt} = N_v A_p \left[ \frac{(L - L_f)RT_{i,0}}{k_1 M_w} + R_s \right]^{-1} (p_{w,i} - p_{w,c}) \quad (41)$$

Finally the total pressure can be calculated taking into account a constant leakage in the chamber and the initial partial pressure of inert gases:

$$p_c = p_{w,c} + p_{in,c} = p_{w,c} + F_{leak} t + p_{in,c,0} \quad \text{for } t \geq t_0 \quad (42)$$

$$p_{w,c} \Big|_{t=0} = p_{c,0} - p_{in,0} \quad \text{for } t = t_0 \quad (43)$$

Partial pressure of the inert gas at the beginning of the PRT has to be taken into account when insert gas is present in chamber atmosphere, and it has to be measured in order to be included in eqs. (42)-(43).

In order to solve eq. (41) the temperature of the vapour in the chamber must be known but, as discussed before, this is not easy to do, as the most reliable methods are the spectroscopic ones; it has been proposed to get the gas temperature in the chamber from thermocouples placed in various positions<sup>[48]</sup>, but great attention to possible bias must be paid. In case the value of  $T_c$  is not available, it can be substituted with the product temperature at the interface of sublimation, or taking an average between  $T_i$  and  $T_s$ , usually committing a small error, as it has been previously discussed.

The actual thickness of the frozen layer is determined through a material balance written across the moving interface, which is solved contemporaneously to the previous equations. The water vapor flow rate at the interface is equal to the difference between the rate of disappearance of the frozen mass and the rate of formation of the dried mass, according to the

following equation:

$$J_w = N_v \left( \rho_f A_p \frac{dL_f}{dt} - \rho_d A_p \frac{dL_f}{dt} \right) \quad (44)$$

The material balance at the interface can be integrated in time between the previous PRT and the actual one, obtaining:

$$L_f = L_f^{(-1)} - \frac{M_w}{R(\rho_f - \rho_d)} \int_{t_0^{(-1)}}^{t_0} \left( \frac{k_1}{T_i} \frac{p_{w,i} - p_{w,c}}{L - L_f} \right) dt \quad (45)$$

where the superscript “(-1)” refers to quantities calculated or measured in the previous PRT.

The integral on the right hand side can be solved applying the trapezoidal rule of integration:

$$L_f = L_f^{(-1)} - \frac{M_w}{R(\rho_f - \rho_d)} \left[ \left( \frac{k_1}{T_{i,0}} \frac{p_{w,i,0} - p_{w,c,0}}{L - L_f} \right) + \left( \frac{k_1^{(-1)}}{T_{i,0}^{(-1)}} \frac{p_{w,i,0}^{(-1)} - p_{w,c,0}^{(-1)}}{L - L_f^{(-1)}} \right) \right] \cdot \frac{t_0 - t_0^{(-1)}}{2} \quad (46)$$

The steps of the DPE algorithm are thus the followings:

- 1) Initial guess of  $T_{i0}$ ,  $k_1$ .
- 2) Determination of  $L_f$  using eq. (46); the values measured and computed in the PRT run at time  $t = t_0^{(-1)}$  are required.
- 3) Determination of  $K_v$  using eq. (40).
- 4) Determination of the initial temperature profile in the frozen product using eq. (37).
- 5) Integration of the system of algebraic-differential equations describing pressure rise in the time interval  $(t_0, t_f)$ , where  $t_f - t_0$  is the time duration of the PRT.
- 6) Repetition of points 2)-5) and determination of the values of  $T_{i,0}$  and  $k_1$  that best fit the calculated chamber pressure ( $p_c$ ) to the measured data ( $p_{c,meas}$ ). The stopper resistance  $R_s$  is dependent only on its geometry, and is supposed to be known; but, eventually, it can be recovered by extrapolation from the values of mass transfer resistance, or experimentally, with a pure water run.

## List of Figures

Figure 1 Comparison between the time evolution of the pressure in the drying chamber (l.h.s.) and of the temperature at the bottom of the product (r.h.s.) calculated for PRTs carried out at 25% (upper graphs), 50% (middle graphs) and 75% (lower graphs) of the primary drying, taking into account the glass wall of the vial (dashed lines,  $K_v = 13.8 \text{ W m}^{-2}\text{K}^{-1}$ ) and using an effective heat transfer coefficient (solid lines,  $K_{v,eff} = 17.7 \text{ W m}^{-2}\text{K}^{-1}$ ). The vials are assumed to be perfectly shielded (time is set equal to zero at the beginning of the PRT).

Figure 2 Comparison between the time evolution of the pressure in the drying chamber (l.h.s.) and of the temperature at the bottom of the product (r.h.s.) calculated for PRTs carried out at 25% (upper graphs), 50% (middle graphs) and 75% (lower graphs) of the primary drying, taking into account radiation from the upper tray (dashed lines,  $K_v = 13.8 \text{ W m}^{-2}\text{K}^{-1}$ ) and using an effective heat transfer coefficient (solid lines,  $K_{v,eff} = 19.0 \text{ W m}^{-2}\text{K}^{-1}$ ). The role of glass wall is neglected (time is set equal to zero at the beginning of the PRT).

Figure 3 Comparison between the time evolution of the pressure in the drying chamber (l.h.s.) and of the temperature at the bottom of the product (r.h.s.) calculated for PRTs carried out at 25% (upper graphs), 50% (middle graphs) and 75% (lower graphs) of the primary drying, taking into account the influence of the pressure on  $K_v$  (dashed lines) and neglecting it (solid lines). The role of glass wall is neglected and the vials are assumed to be perfectly shielded (time is set equal to zero at the beginning of the PRT).

Figure 4 Comparison between the simulated (solid line) and the estimated values ( $\diamond$ : MTM,  $\Delta$ : PRA,  $\square$ : DPE) of the temperature at the interface of sublimation (upper graph, l.h.s.), of the temperature at the bottom of the product (upper graph, r.h.s.), of the sublimation flow (lower graph, l.h.s.), and of the heat transfer coefficient between the shelf and the bottom of the vial (lower graph, r.h.s.). The duration of each PRT is 30 s and the time interval between two PRTs is 30 min; data are collected using a sampling frequency of 10 Hz.

Figure 5 Comparison between the values of  $T_i$  (left hand graphs), of  $J_w$  (right hand side, upper graph), and of  $K_v$  (right hand side, lower graph) obtained by means of mathematical simulation (solid lines) and estimated by means of DPE algorithm for various durations of the PRT ( $\square$ : 30 s,  $\Delta$ : 10 s,  $\circ$ : 5 s). The time interval between two PRTs is 30 min; data are

collected using a sampling frequency of 10 Hz.

Figure 6 Condition number vs. temperature of the sublimating interface and product resistance (left hand side). The contour plot is shown in the right hand side (dashed lines identify the contour lines). The solid lines identify the trajectory of the system in the case study analyzed (curve A, constant shelf temperature), and when the shelf temperature is changed in order to maintain the interface temperature equal to  $-40^{\circ}\text{C}$  (curve B). The duration of the PRT is 30 s in the upper graphs and 5 s in the lower graphs; the time interval between two PRTs is 30 min.

Figure 7 Comparison between the simulated values (solid line) and the values estimated by DPE algorithm ( $\square$ : 2 parameters,  $\blacksquare$ : 1 parameter) of  $T_i$  (upper graph) and of  $L_f$  (lower graph). The duration of each PRT is 30 s, the time interval between two PRTs is 30 min; data are collected using a frequency of 10 Hz.

Figure 8 Comparison between the estimated values ( $\diamond$ : MTM,  $\Delta$ : PRA,  $\square$ : DPE,  $\blacksquare$ : DPE<sup>+</sup>) of the temperature at the interface of sublimation (lower graph, l.h.s.), of the sublimation flow (upper graph, r.h.s.), and of the heat transfer coefficient between the shelf and the bottom of the vial (lower graph, r.h.s.) during the freeze-drying of a 10% by weight sucrose solution ( $p_c = 10 \text{ Pa}$ ,  $d_v = 14.25 \cdot 10^{-3} \text{ m}$ ,  $N_v = 175$ ,  $V_c = 0.2 \text{ m}^3$ ). The duration of each PRT is 30 s; the time interval between two PRT is 30 min. The ratio between the signals of the Pirani and of the Baratron sensors (upper graph, l.h.s.) and the shelf temperature (middle graph, l.h.s.) are also shown. Experiments carried out in *LyoBeta 25* freeze-dryer by Telstar, with *LyoDriver* automatic control.

Figure 1

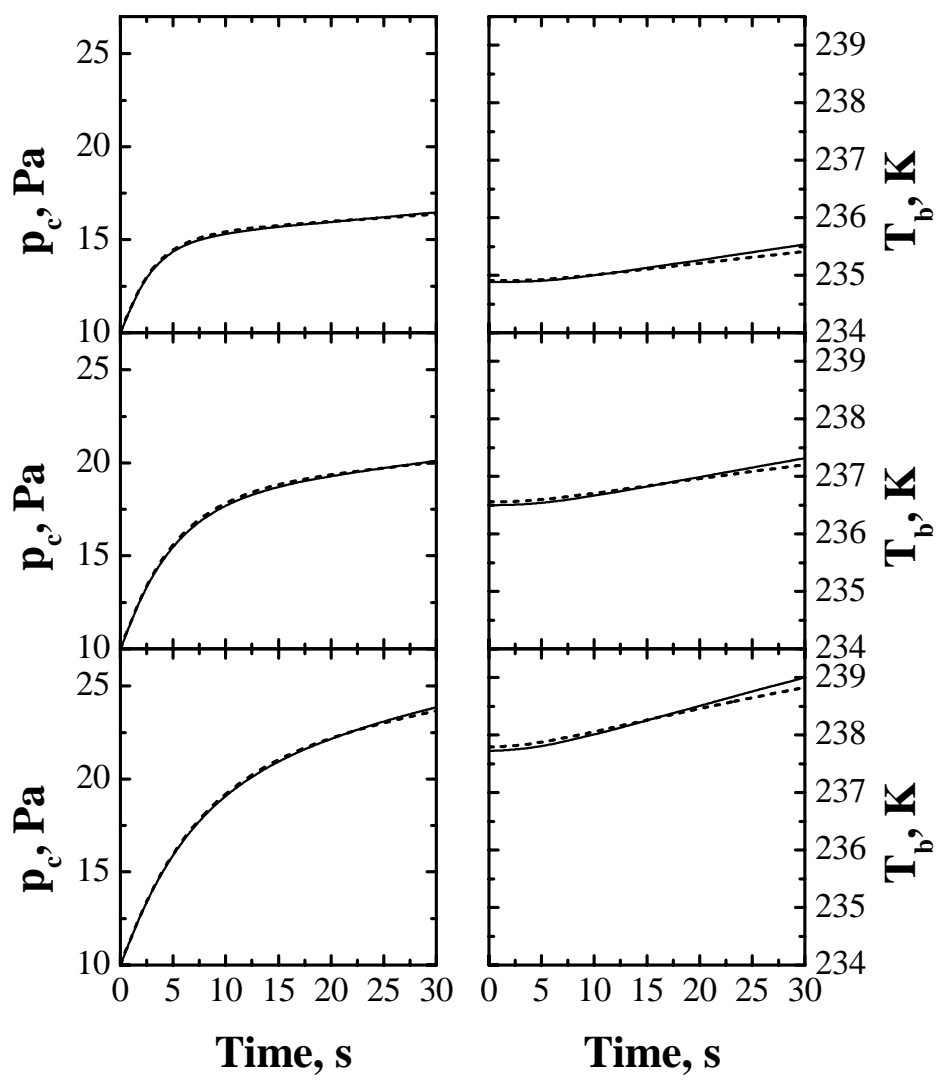




Figure 2

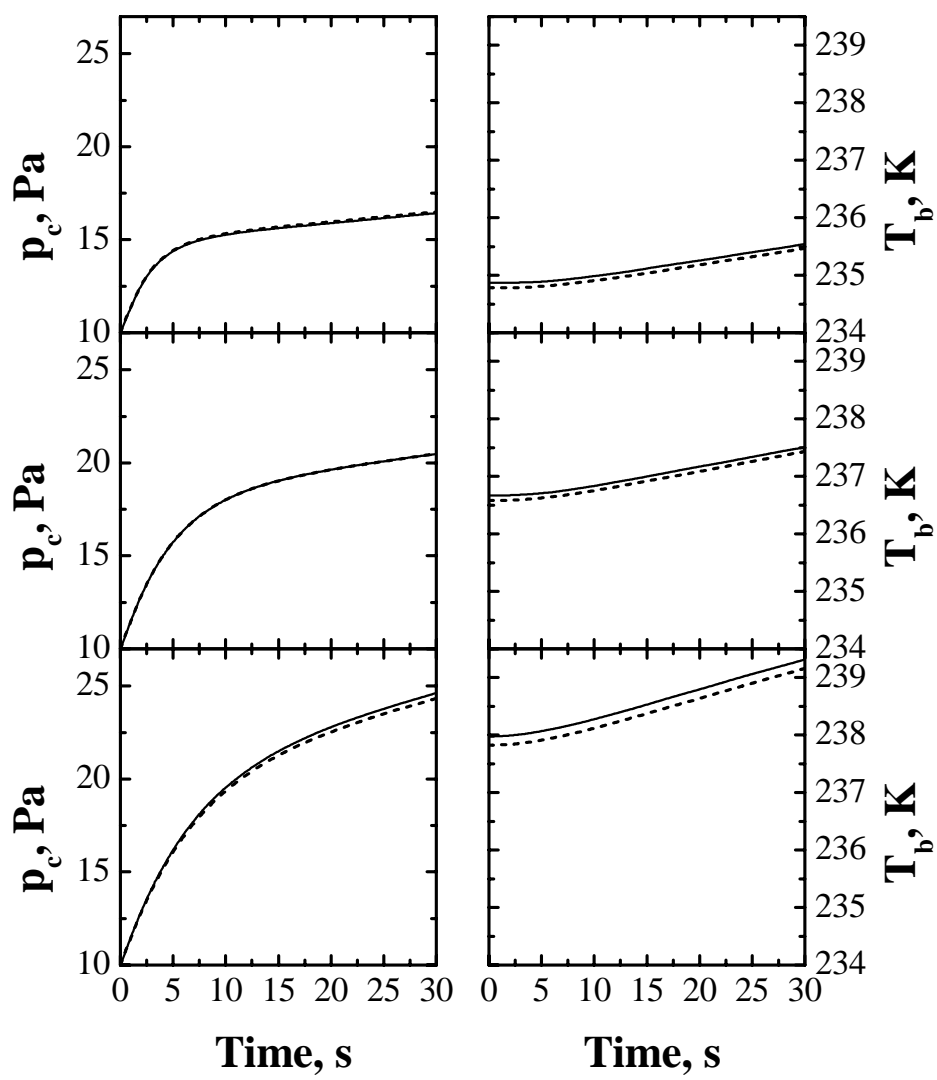


Figure 3

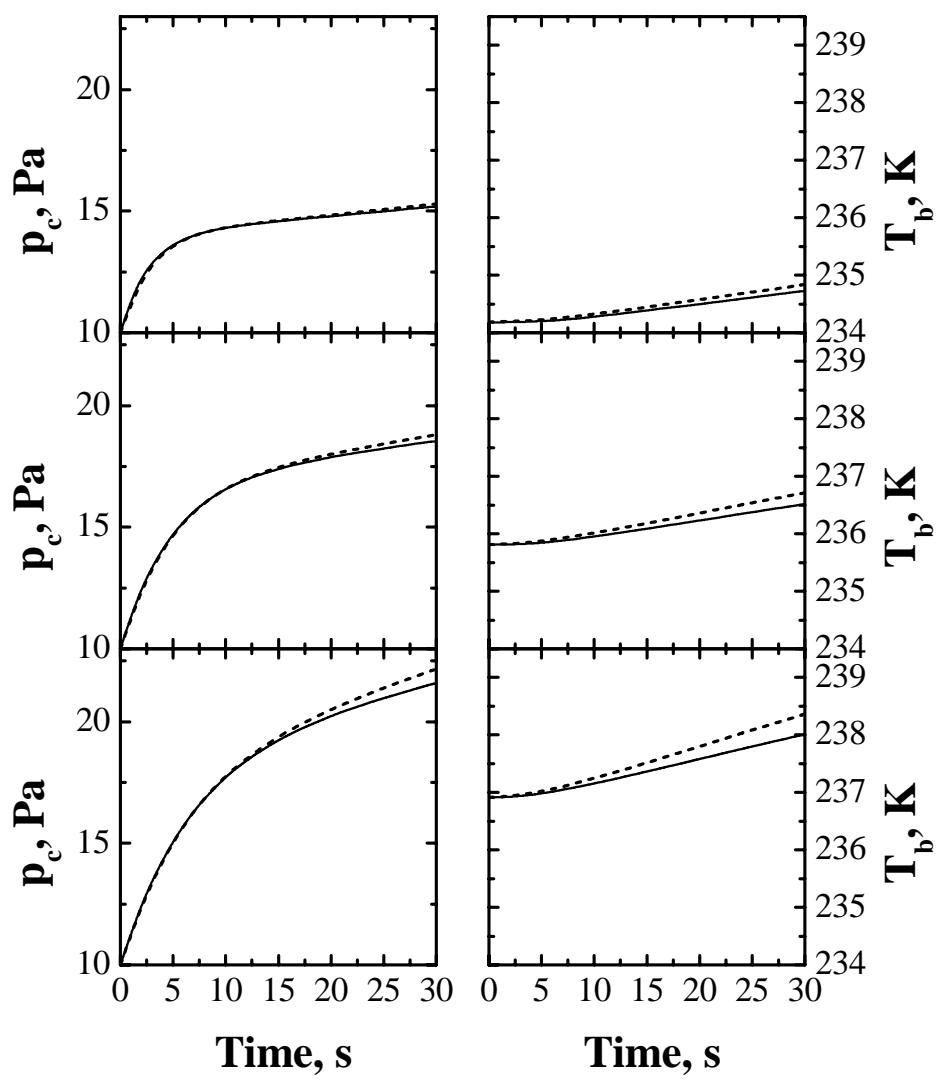


Figure 4

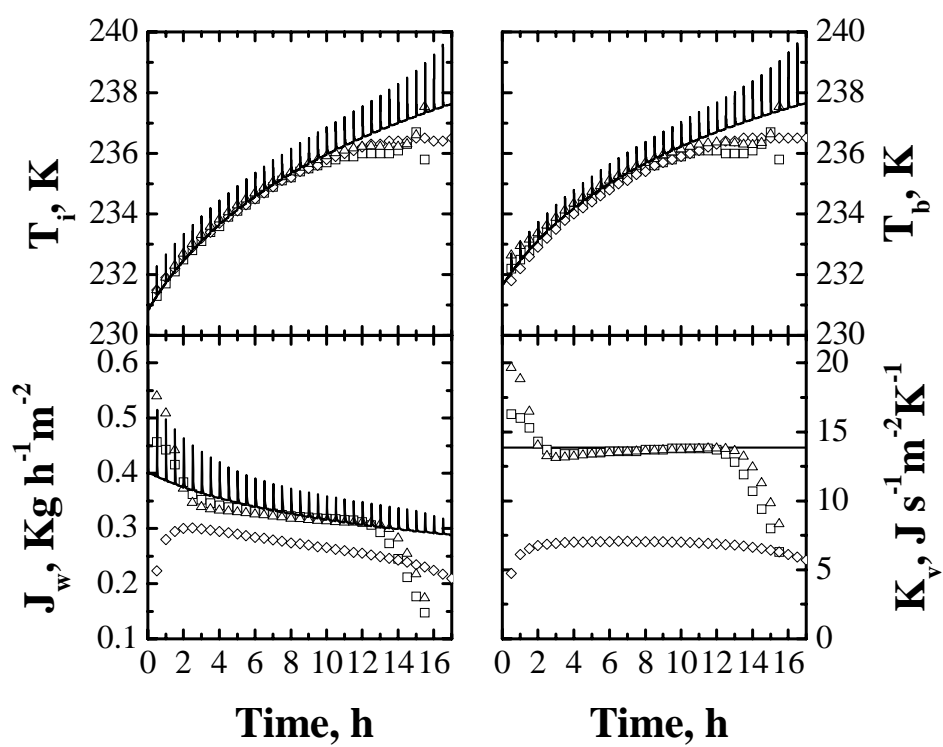


Figure 5

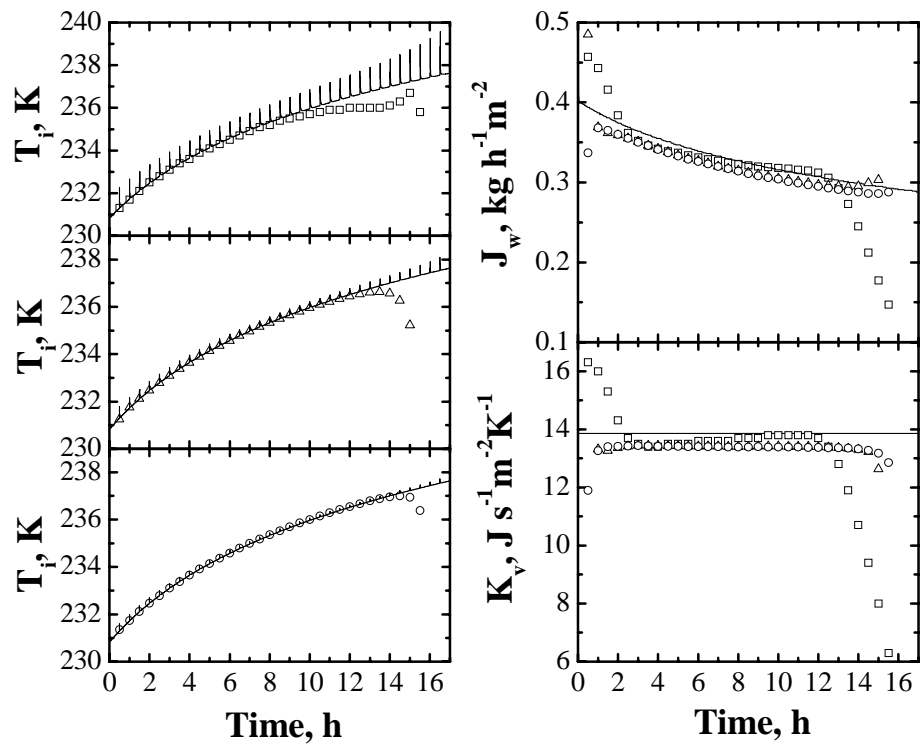


Figure 6

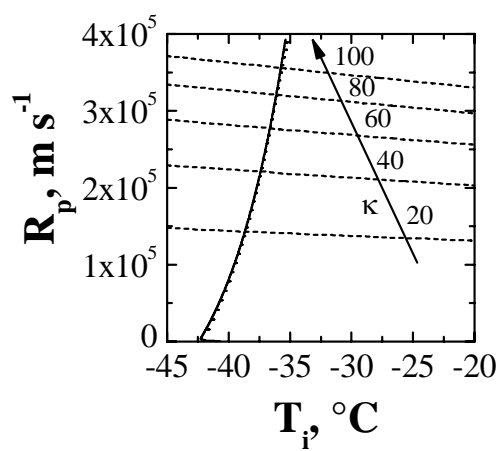
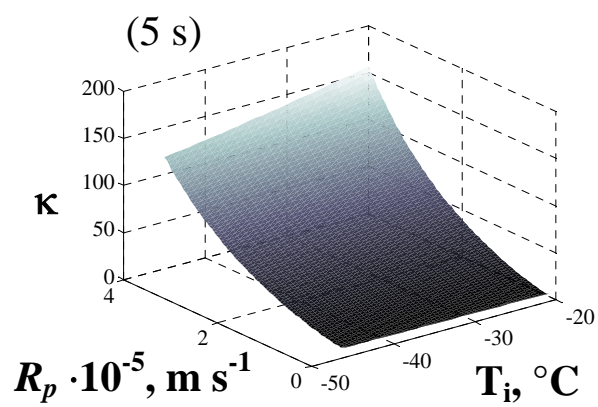
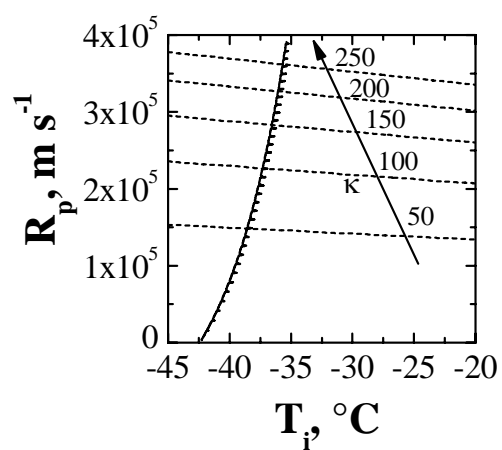
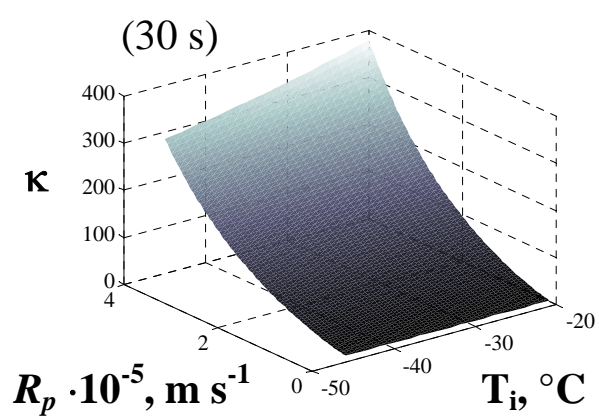


Figure 7

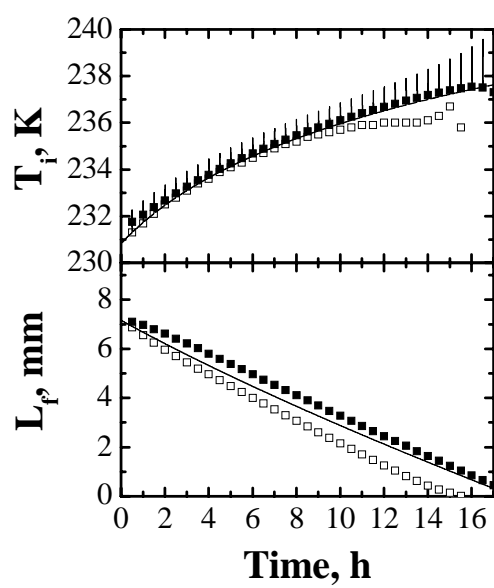


Figure 8

